

Comparison of Transceiver and C+L Band Upgrades: Network Traffic and Energy Assessment

Original

Comparison of Transceiver and C+L Band Upgrades: Network Traffic and Energy Assessment / Sadeghi, Rasoul; DE ARAUJO CORREIA, BRUNO VINICIUS; Virgillito, E.; Napoli, A.; Costa, N.; Pedro, J.; Curri, V.. - ELETTRONICO. - (2021), pp. 1-6. ((Intervento presentato al convegno 3rd International Conference on Electrical, Communication and Computer Engineering, ICECCE 2021 tenutosi a Kuala Lumpur, Malaysia nel 2021 [10.1109/ICECCE52056.2021.9514166]).

Availability:

This version is available at: 11583/2927959 since: 2021-09-29T10:44:02Z

Publisher:

Institute of Electrical and Electronics Engineers Inc.

Published

DOI:10.1109/ICECCE52056.2021.9514166

Terms of use:

openAccess

This article is made available under terms and conditions as specified in the corresponding bibliographic description in the repository

Publisher copyright

IEEE postprint/Author's Accepted Manuscript

©2021 IEEE. Personal use of this material is permitted. Permission from IEEE must be obtained for all other uses, in any current or future media, including reprinting/republishing this material for advertising or promotional purposes, creating new collecting works, for resale or lists, or reuse of any copyrighted component of this work in other works.

(Article begins on next page)

Comparison of Transceiver and C+L Band Upgrades: Network Traffic and Energy Assessment

Rasoul Sadeghi*, Bruno Correia*, Emanuele Virgillito*, Antonio Napoli[†], Nelson Costa[‡],
João Pedro^{‡§} and Vittorio Curri*

* Department of Electronics and Telecommunications (DET)
Politecnico di Torino, Corso Duca degli Abruzzi, Torino, Italy
Email: {rasoul.sadeghi, bruno.dearaujo, emanuele.virgillito, vittorio.curri}@polito.it

[†] Infinera, Sankt-Martinstr. 76, 81541, Munich, Germany
Email: ANapoli@infinera.com

[‡] Infinera Unipessoal Lda, Rua da Garagem 1, 2790-078 Carnaxide, Portugal
Email: {NCosta, JPedro}@infinera.com

[§] Instituto de Telecomunicações, Instituto Superior Técnico, Avenida Rovisco Pais 1, 1049-001 Lisboa, Portugal

Abstract—Being as power-efficient as possible is becoming an issue of increasing importance in optical networks due to the continuous increase of requested capacity resulting from the exponential growth of IP traffic. In this work, we investigate the trade-off between network capacity and energy consumption in optical transport networks when considering (i) three coherent transceiver implementations; (ii) two capacity upgrade strategies, and (iii) uniform and nonuniform traffic distributions. We show that, in Deutsche Telekom (DT) reference network, a nonuniform traffic distribution leads to an increase in network capacity of about 100 Tbps with respect to the uniform case. Interestingly, the nonuniform traffic distribution showed that, in the DT reference network, more traffic could be transmitted with less energy consumption than when considering the uniform traffic distribution. Additionally, it is also shown that C+L systems lead to an only negligible increase in energy consumption while attaining comparable network capacity as adding a second optical fiber and using C-band only for the three considered coherent transceiver implementations. Newer transceivers are found to be very power efficient when compared with older ones. This is a consequence of technological advances enabling to increase capacity via using higher-order modulation formats and baud rates. In the case of the ZR implementation, a compromise between lower power consumption and capacity was reached to address shorter links.

Index Terms—Optical fiber communication, multi-band, transmission modeling, optical amplification

I. INTRODUCTION

To cope with the continuous increase of network traffic boosted, for example, by the worldwide COVID-19 pandemic [1] and simultaneously limit the overall power consumption of telecommunication networks [2], high capacity as well as power-efficient transceivers (TRXs) are required. Furthermore, to increase the capacity of Wavelength-Division Multiplexing (WDM) systems – that nowadays operate in C-band only with a spectrum of around 4.8 THz – two techniques have been proposed: (a) spatial division multiplexing (SDM) and (b) band division multiplexing (BDM) [3]. The latter aims to exploit the full low-loss spectrum of the widely deployed ITU-T G.652.D optical fiber, which exceeds 50 THz [4]–[6], by exploiting the benefits of the other single-mode bands.

BDM, not only cost-effectively increases network capacity [4], but also has the potential to reduce the capital expenditure (CAPEX). On the contrary, the SDM approach relies on the availability of dark fibers or on the deployment of new ones. Some analyses have already been carried out regarding the power consumption of TRXs. In [7], the authors showed that the scaling of Intel’s integrated circuit CMOS node size is decreasing every two years. Moreover, the availability of digital signal processing application-specific integrated circuit (DSP ASIC)s at the respective CMOS node size has been shown in several other works [8]–[10]. The CMOS power consumption depends on the node size, with an energy reduction of $\sim 30\%$ in each process step [11]. In 2013, the Optical Internetworking Forum (OIF) defined an implementation agreement (IA) for the application of coherent techniques in pluggable form factors [12]. One of the latest IAs is the 400ZR [13], which defines a power-efficient and cost-effective coherent interface to support 400 Gbps using the symbol rate of 59.84 Gbaud. In [12], the authors analyzed how coherent DSP and ASICs scale with power dissipation and developed a model to predict data rates as well as energy consumption of TRXs based on coherent transmission technology. In this work, we perform a statistical network assessment [14] over DT network topology with uniform [5] and nonuniform [6] traffic distributions. We compare the performances of three different coherent transceiver implementations applied together with BDM or SDM. For BDM, we consider both the L- and C-band, while, for SDM, we activate an additional dark fiber operating on the C-band only. Moreover, for SDM, we assume the Core Continuity Constraint (CCC), which is enforced by the reconfigurable optical add-drop multiplexer (ROADM) [15]. Results highlight that BDM (C+L-band transmission) leads to comparable performance as SDM (with two fibers), with the latter exhibiting just a minor advantage with respect to network capacity and energy efficiency. This observation supports that BDM is a cost-effective capacity upgrade strategy. Furthermore, the dependence of energy efficiency on traffic load is shown to be similar for all analyzed cases.

II. METHODOLOGY

In this work, we modeled a light path (LP) based on two Gaussian disturbances: amplified spontaneous emission (ASE) noise and nonlinear interference (NLI), introduced by the amplifiers and fiber propagation, respectively. To this end, the quality of transmission (QoT) at the end of each fiber span can be estimated by the generalized signal-to-noise ratio (GSNR) [5]. The ASE noise power can be calculated as given in Eq. 1.

$$P_{ASE,i} = hf_i NF(f_i) G(f_i) B_{ref} \quad (1)$$

where h is the Planck's constant, B_{ref} is the reference bandwidth, and $G(f_i)$ and $NF(f_i)$ are the gain and noise figures of the amplifiers in f_i , respectively. The Generalized Gaussian Noise (GGN) model is used to calculate the nonlinear (NLI) contribution of fiber transmission [16], [17]. The effects of spectral and spatial variations of fiber loss as well as the spontaneous Raman scattering (SRS)-induced [18] inter-channel power crosstalk have been considered. As a result, the NLI power is given by:

$$P_{NLI,i} = G_{NLI}(f_i) B_{ref} \quad (2)$$

in Eq. 2, the NLI power spectral density ($G_{NLI}(f_i)$) is presented. By using the described methodology, the Generalized Signal-to-Noise Ratio (GSNR) for a single span can be calculated as:

$$GSNR_i = \frac{P_{S,i}}{P_{ASE,i} + P_{NLI,i}} = (\text{OSNR}_i^{-1} + \text{SNR}_{NL,i}^{-1})^{-1} \quad (3)$$

$$GSNR_{i,l} = \frac{1}{\sum_{s \in l} (\text{GSNR}_{i,s})^{-1}} \quad (4)$$

In eq. 3, $P_{S,i}$ indicates the fiber input power, and OSNR_i and $\text{SNR}_{NL,i}$ are the optical signal-to-noise ratio (OSNR) and NLI signal-to-noise ratio, all evaluated for the i -th channel under test. After evaluating the GSNR of a single span, we can use Eq. 4 to find the total GSNR of a LP l in the i -th frequency channel. The GSNR profile has been depicted in Fig. 1, which transmission over ITU-T G.652D fiber with a uniform span length of 75 km is assumed. Erbium-doped

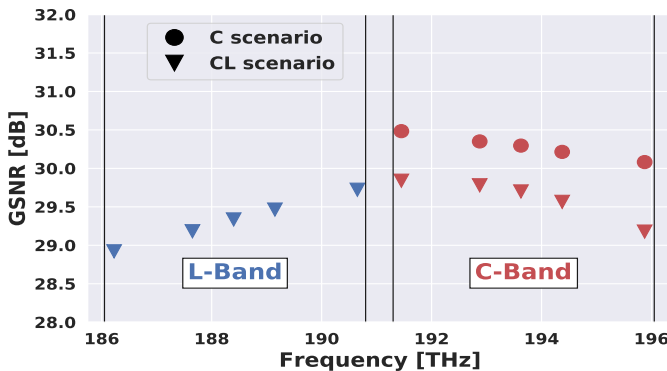


Fig. 1: GSNR profiles for a single 75 km span in C and C+L band transmission.

fiber amplifier (EDFA) lumped amplification is considered for both C- and L-bands [19], with the fiber losses being fully compensated at the end of each fiber span. Moreover, average noise figures of 4.25 and 4.68 dB are considered for the EDFAs in C- and L-band, respectively. 64 channels deployed in each band, where each channel is allocated a 75 GHz frequency slot. Line interfaces are applied to operate at a symbol rate of 64 Gbaud; and, a 500 GHz guard band is imposed between C- and L-bands. The Locally Optimized Globally Optimized (LOGO) approach is used for optical power optimization, which indicates the optimum launch powers of -2.11 dBm for the C- and -1.99 dBm for the L-band in the aforementioned conditions per span. As a result, the average GSNR for the C-band only system (i.e., assuming the L-band is not used) is 30.28 dB with a minimum GSNR of 30.08 dB and the maximum GSNR of 30.48 dB; however, if both bands are used, the average GSNR is decreased to 29.61 dB with the minimum and maximum GSNR values of 29.17 and 29.83 dB, respectively, in the C band, and 29.32 dB with the minimum and maximum GSNR values of 28.92 and 29.72 dB, respectively in the L-band. This result highlights that, due to the SRS effect, the QoT in the C-band decreases by about 1 dB when enabling the L-band.

III. DATA AND NETWORK ANALYZES

The DT network topology with 17 nodes and 26 links [6] is considered in this work. A disaggregated abstraction of the physical layer based on the GSNR as QoT criteria is exploited in this network [20], [21]. As detailed in the previous section, the launched optical power is first optimized to maximize the GSNR [22], which calculated by using the open source library GNPY [23]. Then, we apply the Statistical Network Assessment Process (SNAP), which is a Monte-Carlo based software, to derive networking, traffic and energy metrics [14]. The network is progressively loaded with traffic following either a uniform or a nonuniform Joint Probability Density Function (JPDF) [6]. The number of Monte-Carlo in the SNAP considered equal to 30000, with the best GSNR wavelength assignment policy. The K -shortest path algorithm being used with $K_{max} = 15$ as the number of alternative shortest paths between source and destination nodes.

Three different transceivers are manipulated in the network in order to assess the behavior of it in terms of capacity and energy consumption. Table I reports the capacity and energy consumption for the three considered TRX implementations (considering the operation of each TRX with different data rates and distances): TRX Flex Format 16 (FF16) [12] models a TRX from the year 2016; FF20 is the prediction for a standard TRX in the year 2020 [12] and, finally, the ZR TRX is defined as 400ZR IA of OIF [24].

As shown in Table I, the ZR TRX supports 16QAM, 8QAM, and QPSK modulation formats only¹. However, FF16 was supporting 32QAM, and based on this scenario, it has assumed

¹400ZR IA defines only 400G transmission with 16QAM < 120km. Nevertheless, it is a common assumption in the industry that the other modes will be possible and this is often designated as OpenZR+.

TABLE I: TRXs modelling assumptions.

TRX	mod. form.	Data rate [Gb/s]	Typical Reach [km]	P[W]
ZR [24]	16QAM	400	$L < 120$	15
	16QAM	400	$120 < L < 450$	20
	8QAM	300	$450 < L < 1500$	18
	QPSK	200	$1500 < L < 2500$	16
	QPSK	100	$2500 < L$	13
FF16 [12]	32QAM	500	$L < 200$	42.5
	16QAM	400	$200 < L < 1000$	38
	8QAM	300	$1000 < L < 2000$	35
	QPSK	200	$2000 < L < 4000$	32
	QPSK	100	$4000 < L$	35
FF20 [12]	32QAM	500	$L < 600$	27
	16QAM	400	$600 < L < 1500$	22
	8QAM	300	$1500 < L < 3500$	20
	QPSK	200	$3500 < L < 6000$	18
	QPSK	100	$6000 < L$	50

FF20 will support also 32QAM for shorter reach applications in [12]. Consequently, a maximum data rate of {400, 500, 500} Gb/s are attainable by ZR, FF16, and FF20 TRXs, respectively. Although operation at about 64 Gbaud only is assumed in this work, operation at smaller baud rate is still possible when using these TRXs to enhance the reach or improve spectral efficiency. An example of such operation is depicted in Table I by 100 Gb/s QSPK, which operates at about 32 Gbaud. A maximum energy consumption of 20 W is assumed for ZR TRX, when using 16QAM modulation format to reach a distance between 120 km and 450 km. For FF16, a maximum power consumption of 42.5 W is attained when using the most aggressive modulation format (32QAM) designed for short distances, i.e., < 200 km. On the contrary, the maximum predicted energy consumption for FF20 is 50 W which is reached when using QPSK modulation format to bridge distances exceeding 6000 km; as a consequence of the increase of DSP power requirements to compensate for the transmission effects, such as the accumulated chromatic dispersion. Please note that both FF16 and FF20 TRXs are assumed to have a FEC overhead of 28%, but this parameter decreases to 15% for ZR TRX. During operation, the optimal modulation format with respect to the distances that they support is selected with taking into account the LP QoT. The Required OSNR (ROSNR) for each modulation format is investigated in [25]. Here, they present a ROSNR in back-to-back operation (B2B) for different modulation formats, {14, 18, 21, 25} dB for QPSK, 8QAM, 16QAM, and 32QAM, respectively.

IV. RESULTS

In this section, we analyze the impact of using three different TRXs implementations on the analyzed topology (DT) in terms of network capacity and energy consumption when employing SDM-CCC ($2 \times$ fiber) and BDM upgrade (C+L band) strategies with two different JPDFs for the traffic distribution. In the case of SDM-CCC, we assume C-band transmission only in both fibers; however, in the case of BDM, we propose to allocate channels also in the L-band. It is worth

mentioning that the number of channels in the C and L band is considered as the same number, 64, in order to have a meaningful comparison between SDM and BDM upgrades.

Turning to the results, Figures 2(a) and (b) show the blocking probability (BP) versus total allocated traffic when considering single-fiber C-band only transmission (*ref*), *SDM*, and *BDM* for both uniform and nonuniform JPDF traffic distributions. It is observable that FF20 TRX at this network leads to the largest total allocated traffic in all scenarios in comparison to the other TRX implementations. This is a consequence of supporting the more spectral efficient modulation formats – 32QAM –, while, also having better optical performance (i.e. longer reach) in comparison to the both of FF16 and ZR. Next, the TRX of FF16 provides a capacity between ZR and FF20 TRXs implementations. Figures 2(a) and (b) also show that the capacity of the network is similar when using the SDM-CCC ($2 \times$ fibers in C-band) and BDM (single fiber in C+L-band) upgrade strategies for all analyzed TRX implementations. Indeed, for the same blocking probability, the difference in the allocated traffic between SDM and BDM upgrades is always negligible. For instance, in the FF20 TRX the difference of allocated traffic between SDM and BDM at blocking probability of 1% is 5.6 Tbps and 2.3 Tbps for uniform and nonuniform JPDFs, respectively. Fig. 2(c) is prepared to better explanation of the network behavior in different upgrades. This figure shows the capacity of the DT network as well as the traffic multiplicative factor, i.e., the ratio of allocated traffic in BDM (or SDM) with respect to the reference case at $BP = 1\%$ with uniform and nonuniform JPDF for the traffic distribution. The analysis of Fig. 2(c) shows that the network capacity increases by about 100 Tbps in the nonuniform case in comparison with the uniform traffic distribution. The reason of network capacity increasing with nonuniform JPDF is the proximity of densely populated cities (nodes) at this network. Therefore, distances between nodes will be decreased, consequently wavelength continuity would be increase and most efficient modulation formats will be used. Moreover, both BDM and SDM upgrade strategies

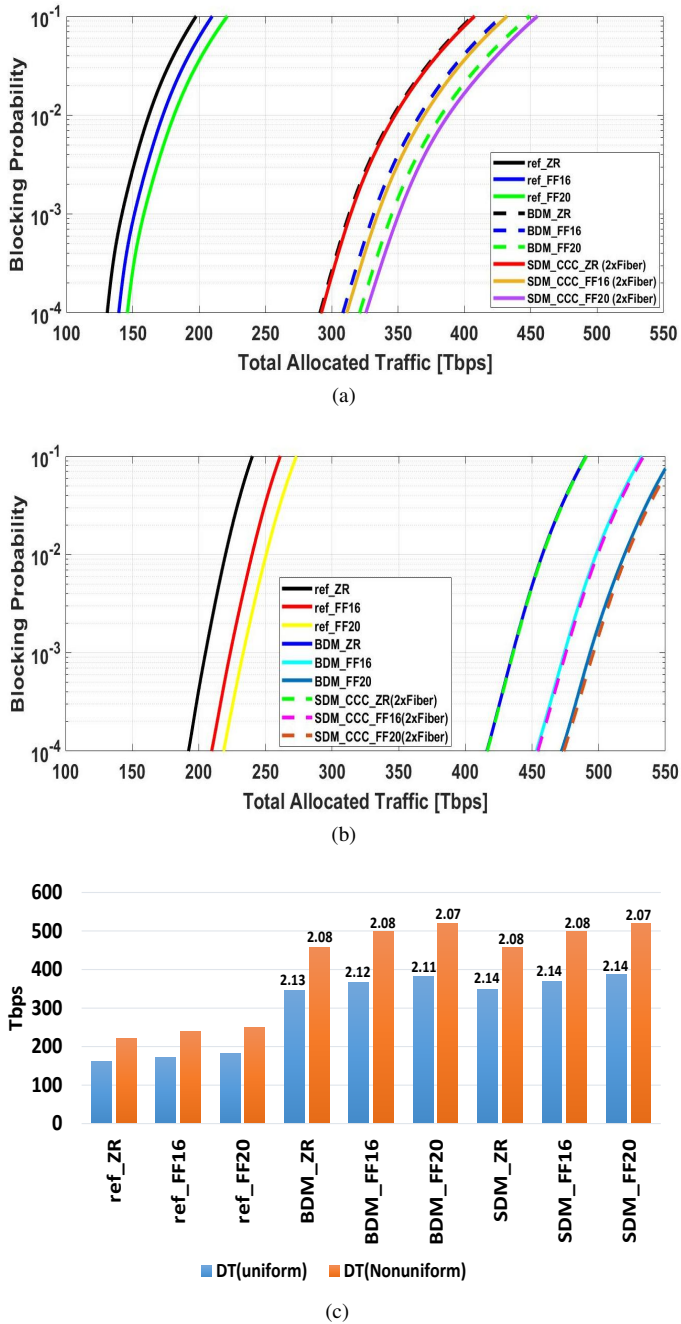


Fig. 2: (a) uniform (b) Nonuniform - BP versus allocated traffic, respectively, and (c) capacity (multiplicative factor inset) for each upgrade at BP = 1% for DT topology.

perform similarly, showing a comparable multiplicative factor, exceeding 2, for all cases. This value can be explained by the increase in the number of available wavelengths, i.e., two times in both BDM and SDM-CCC, which results in a benefit in terms of statistical multiplexing when searching for available wavelength resources. It is worth mentioning that the small difference between SDM and BDM results mainly from the different of obtained QoT in the two scenarios. In other words,

the QoT in the BDM upgrade is ≈ 1 dB less in comparison to the C band only which is used in SDM-CCC upgrade.

After capacity investigation in DT network by using SDM and BDM upgrades, energy consumption analyzed to show a comprehensive comparison between two upgrades. Figure 3 presents the energy consumption in Joule per bit (Jpb) when considering both uniform and nonuniform JPDF for traffic distribution. The results show that SDM for capacity upgrade consumes slightly lower total energy consumption in comparison to the BDM upgrade. Moreover, for all TRX implementations, the power consumption (required Jpb) remains mostly independent of the traffic load until a specific load (250 Tbps). For instance, {17.27, 20.13, 17.76} dBjpb in SDM and {17.28, 20.16, 17.78} dBjpb in BDM upgrade for ZR, FF16 and FF20 TRXs, respectively. This result means that, to send a bit in the DT network, the network operator has to support a fixed energy consumption for each bit until reaching this specific traffic load (250 Tbps). After that threshold (250 Tbps), the required energy can grow sharply (e.g. see Fig. 3(a)), because the network starts to saturate, leading to the need to resort to longer lightpaths (LP). This, in turn, leads to the use of less spectral efficient modulation formats, which implies that more transceivers are required to fulfill the traffic requirements. Importantly, the described behavior also depends on the TRX implementation. For instance, the better performing FF20 only experiences the described behavior for higher traffic loads. As can be seen in Fig. 3 (a) and (b), FF16 and FF20 not only enable increasing the capacity when considering the nonuniform JPDF for traffic distribution, but also lead to a small decrease of the energy consumption. On the contrary, a different behavior is observed with the ZR TRX. In this case, the capacity is still increased in the nonuniform case but the energy consumption also increases slightly from about 17.27 dB to 17.36 dB. This increase in energy consumption in nonuniform JPDF with ZR TRX due to the shortening the LPs (proximity of densely populated cities (nodes) at this network leads to a decrease in the length of requested LPs.) and consequently using the most efficient modulation formats, which their power consumption are high (see Table I); so, energy consumption has grown at this JPDF. In addition, in this topology, the energy consumption penalty between the BDM and SDM-CCC upgrade strategies decreased in the nonuniform JPDF case in comparison with the uniform one. According to Fig. 3, the traffic difference between two BP of 0.1% and 10%, decreased more than 38 Tbps when considering the nonuniform distribution instead of the uniform one. In other words, network saturation speed is increasing when nonuniform JPDF manipulate in the traffic distribution in comparison to the uniform case. In Fig. 3 (a), (b), and (c), the required energy per transferred bit for three different values of BP has been marked with: \otimes , \diamond and \ominus , identifying BP equals to 0.1%, 1% and 10%, respectively. These markers show that, for ZR and FF16 TRX implementations, the energy consumption increases sharply, in the range of 95 Tbps; however, in the nonuniform JPDF, this range decreases to 54.9 Tbps. On the contrary, this difference is 105 Tbps in

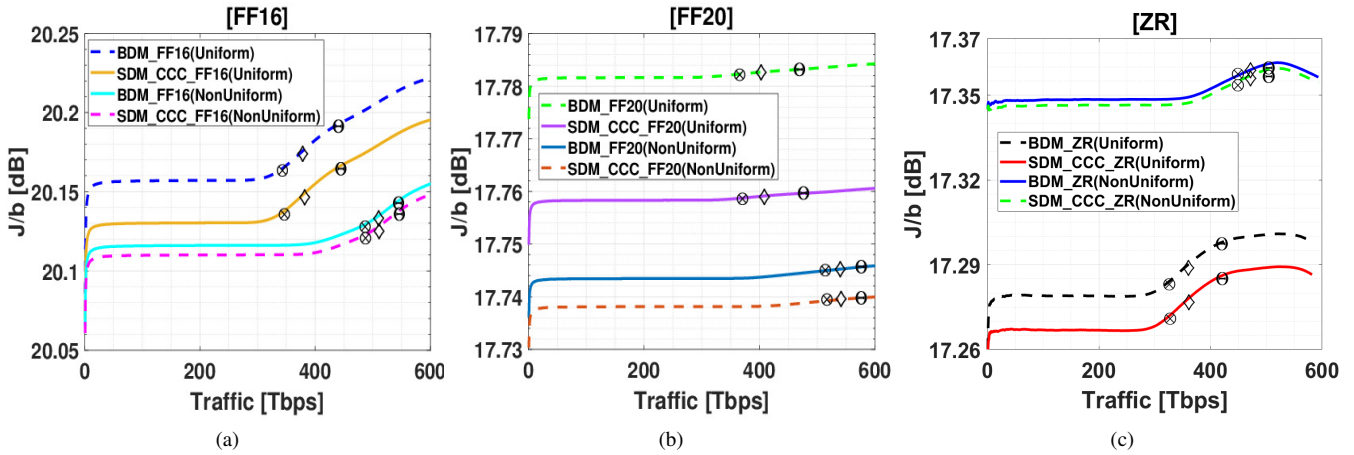


Fig. 3: Energy consumption per bit – as Joule per bit – versus total allocated traffic for (a) FF16, (b) FF20 and (c) ZR TRXs for SDM and BDM with uniform and nonuniform JPFD traffic distribution in DT topology. \otimes , \diamond , and \ominus identify the BP of 0.1%, 1%, and 10%, respectively.

uniform and 62 Tbps in the nonuniform JPFD, more than other TRX implementation in FF20, and the energy consumption changes were smooth in the BP range from 0.1% to 10%.

V. CONCLUSIONS

We analyzed the DT reference networks in terms of capacity and energy consumption per bit for two SDM-CCC ($2 \times$ fiber) and BDM (C+L-band) capacity upgrade strategies by employing ZR, FF16 and FF20 transceiver implementations. We showed that adding the L-band to a C-band system has practically the same effect on the network capacity as using a second dark fiber making use of C-band-only. Moreover, a traffic multiplicative factor exceeding 2 times was found for both upgrade strategies. Furthermore, we investigated the impact of each TRX implementation in the network when applying uniform and nonuniform JPFD for traffic distribution. Although both upgrade strategies extend the capacity of networks by more than two times, it was observed that changing the JPFD from uniform to nonuniform leads to increase the network capacity about 100 Tbps. With respect to energy efficiency, both SDM and BDM solutions behave similarly with a given gap between each TRX implementation, which results naturally from their different characteristics (modulation formats supported, typical reach, and power consumption). Moreover, we show that the energy consumption normalized to the carried traffic load shows a constant value in both networks until a specific threshold traffic load related to capacity exhaustion. Above this value, the need to route traffic over longer paths results in the use of less spectral efficient modulation formats, consequently increasing the number of optical interfaces and energy consumption.

ACKNOWLEDGMENT

This work was supported by the European Union’s Horizon 2020 research and innovation program under the Marie Skłodowska-Curie ETN WON, grant agreement 814276 and by the Telecom Infra project.

REFERENCES

- [1] OECD, “Keeping the internet up and running in times of crisis,” tech. rep.
- [2] F. Musumeci, M. Tornatore, and A. Pattavina, “A power consumption analysis for ip-over-wdm core network architectures,” *J. Opt. Commun. Netw.*, vol. 4, pp. 108–117, Feb 2012.
- [3] A. Ferrari, E. Virgillito, and V. Curri, “Band-division vs. space-division multiplexing: A network performance statistical assessment,” *Journal of Lightwave Technology*, vol. 38, no. 5, pp. 1041–1049, 2020.
- [4] A. Ferrari, A. Napoli, J. K. Fischer, N. M. S. d. Costa, A. D’Amico, J. Pedro, W. Forsyia, E. Pincemin, A. Lord, A. Stavdas, J. P. Fernandez-Palacios Gimnez, G. Roelkens, N. Calabretta, S. Abrate, B. Sommerkorn-Krombholz, and V. Curri, “Assessment on the achievable throughput of multi-band itu-t g.652.d fiber transmission systems,” *Journal of Lightwave Technology*, pp. 1–1, 2020.
- [5] E. Virgillito, R. Sadeghi, A. Ferrari, G. Borracchini, A. Napoli, and V. Curri, “Network performance assessment of c+l upgrades vs. fiber doubling sdm solutions,” in *Optical Fiber Communication Conference (OFC) 2020*, p. M2G.4, Optical Society of America, 2020.
- [6] E. Virgillito, R. Sadeghi, A. Ferrari, A. Napoli, B. Correia, and V. Curri, “Network performance assessment with uniform non-uniform nodes distribution in c+l upgrades vs. fiber doubling sdm solutions,” in *International Conference on Optical Network Design and Modelling (ONDM) 2020*, 2020.
- [7] W. M. Holt, “1.1 moore’s law: A path going forward,” in *2016 IEEE International Solid-State Circuits Conference (ISSCC)*, pp. 8–13, 2016.
- [8] C. Laperle, “Advances in high-speed adcs, dacs, and dsp for optical transceivers,” in *Optical Fiber Communication Conference/National Fiber Optic Engineers Conference 2013*, p. OTh1F.5, Optical Society of America, 2013.
- [9] D. A. Morero, M. A. Castrillón, A. Aguirre, M. R. Hueda, and O. E. Agazzi, “Design tradeoffs and challenges in practical coherent optical transceiver implementations,” *J. Lightwave Technol.*, vol. 34, pp. 121–136, Jan 2016.
- [10] O. Ishida, K. Takei, and E. Yamazaki, “Power efficient dsp implementation for 100g-and-beyond multi-haul coherent fiber-optic communications,” in *2016 Optical Fiber Communications Conference and Exhibition (OFC)*, pp. 1–3, 2016.
- [11] D. A. Morero, M. A. Castrillón, A. Aguirre, M. R. Hueda, and O. E. Agazzi, “Design tradeoffs and challenges in practical coherent optical transceiver implementations,” *J. Lightwave Technol.*, vol. 34, pp. 121–136, Jan 2016.
- [12] F. Frey, R. Elschner, and J. K. Fischer, “Estimation of trends for coherent dsp ASIC power dissipation for different bitrates and transmission reaches,” pp. 1–8, 2017.
- [13] “OIF 400ZR IA.” https://www.oiforum.com/wp-content/uploads/OIF-400ZR-01.0_reduced2.pdf.

- [14] V. Curri, M. Cantono, and R. Gaudino, "Elastic all-optical networks: A new paradigm enabled by the physical layer. how to optimize network performances?," *Journal of Lightwave Technology*, vol. 35, no. 6, pp. 1211–1221, 2017.
- [15] R. Rumipamba-Zambrano, F.-J. Moreno-Muro, P. Pavón-Marino, J. Perelló, S. Spadaro, and J. Solé-Pareta, "Assessment of flex-grid/MCF optical networks with ROADM limited core switching capability," in *2017 International Conference on Optical Network Design and Modeling (ONDM)*, pp. 1–6, IEEE, 2017.
- [16] M. Cantono, D. Pileri, A. Ferrari, and V. Curri, "Introducing the Generalized GN-model for Nonlinear Interference Generation including space/frequency variations of loss/gain," *Journal of Lightwave Technology*, vol. 36, pp. 3131–3141, oct 2017.
- [17] D. Semrau, E. Sillekens, R. I. Killey, and P. Bayvel, "The isrs gn model, an efficient tool in modeling ultra-wideband transmission in point-to-point and network scenarios," in *2018 European Conference on Optical Communication (ECOC)*, 2018.
- [18] V. Curri, A. Carena, A. Arduino, G. Bosco, P. Poggiolini, A. Nespola, and F. Forghieri, "Design strategies and merit of system parameters for uniform uncompensated links supporting nyquist-wdm transmission," *Journal of Lightwave Technology*, vol. 33, no. 18, pp. 3921–3932, 2015.
- [19] A. Ferrari, A. Napoli, J. K. Fischer, N. M. S. da Costa, A. D'Amico, J. Pedro, W. Forsyiaik, E. Pincemin, A. Lord, A. Stavdas, *et al.*, "Assessment on the achievable throughput of multi-band itu-t g. 652. d fiber transmission systems," *Journal of Lightwave Technology*, 2020.
- [20] V. Kamalov, M. Cantono, V. Vusirikala, L. Jovanovski, M. Salsi, A. Pilipetskii, D. K. M. Bolshtyansky, G. Mohs, E. R. Hartling, and S. Grubb, "The subsea fiber as a Shannon channel," in *In Proceedings of the SubOptic*, 2019.
- [21] V. Curri, "Software-defined wdm optical transport in disaggregated open optical networks," in *ICTON 2020*, p. We.C2.1, IEEE, 2018.
- [22] A. Ferrari, D. Pileri, E. Virgillito, and V. Curri, "Power control strategies in C+ L optical line systems," in *Optical Fiber Communication Conference*, pp. W2A–48, Optical Society of America, 2019.
- [23] "OOPT-GNPy web app." <https://gnpy.app/>. Accessed: 2020-07-01.
- [24] OIF, "Implementation Agreement 400ZR." <https://www.oiforum.com/wp-content/uploads/OIF-400ZR-01.0-reduced2.pdf>.
- [25] J. Pedro and S. Pato, "Capacity increase and hardware savings in dwdm networks exploiting next-generation optical line interfaces," pp. 1–6, 2018.